Molecular Crystals and Liquid Crystals

Publication details, including instructions for authors and subscription information:
http://www.tandfonline.com/loi/gmcl20

RNA-Wrapped Carbon Nanotubes Aggregation Induced by Polymer Hybridization

V. A. Karachevtsev [a], G. O. Gladchenko [a], M. V. Karachevtsev [a], A. Yu. Glamazda [a], V. S. Leontiev [a], O. S. Lytvyn [b] & U. Dettlaff-Weglikowska [c]

[a] B.I. Verkin Institute for Low Temperature Physics and Engineering, Kharkiv, Ukraine

[b] V. Lashkaryov Institute of Semiconductor Physics, Kyiv, Ukraine

[c] Max-Planck Institute for Solid State Research, Stuttgart, Germany

Version of record first published: 10 Jun 2010

To cite this article: V. A. Karachevtsev, G. O. Gladchenko, M. V. Karachevtsev, A. Yu. Glamazda, V. S. Leontiev, O. S. Lytvyn & U. Dettlaff-Weglikowska (2008): RNA-Wrapped Carbon Nanotubes Aggregation Induced by Polymer Hybridization, Molecular Crystals and Liquid Crystals, 497:1, 7/[339]-19/[351]

To link to this article: http://dx.doi.org/10.1080/15421400802458183

Mol. Cryst. Liq. Cryst., Vol. 497, pp. 7/[339]–19/[351], 2008

ISSN: 1542-1406 print/1563-5287 online
DOI: 10.1080/15421400802458183

Taylor & Francis
Taylor & Francis Group

RNA-Wrapped Carbon Nanotubes Aggregation Induced by Polymer Hybridization

V. A. Karachevtsev[1], G. O. Gladchenko[1], M. V. Karachevtsev[1], A. Yu. Glamazda[1], V. S. Leontiev[1], O. S. Lytvyn[2], and U. Dettlaff-Weglikowska[3]
[1]B.I. Verkin Institute for Low Temperature Physics and Engineering, Kharkiv, Ukraine
[2]V. Lashkaryov Institute of Semiconductor Physics, Kyiv, Ukraine
[3]Max-Planck Institute for Solid State Research, Stuttgart, Germany

The aggregation of poly(rA)-wrapped single-walled carbon nanotubes (SWNTs) induced by hybridization of the adsorbed polymer with free poly(rU) has been studied by differential UV absorption spectroscopy, NIR luminescence, and AFM. After the addition of poly(rU) into a poly(rA):SWNTs suspension, the double-stranded poly(rA)·poly(rU) was formed, which is evident from the characteristic S-like form of the melting curve for the polymer created. Hybridization of free poly(rU) with two complementary poly(rA), one of which was adsorbed to different individual nanotubes, links them together and causes the appearance of aggregates. The aggregation of nanotubes is accompanied with light scattering and can be monitored in an AFM image after the deposition of the suspension on a mica substrate. Molecular dynamic simulation demonstrates a possible structure of the SWNTs aggregate.

Keywords: adsorption; aggregation; hybridization; nanotubes; nucleic acids

1. INTRODUCTION

SWNTs as a promising nanomaterial with unique physical properties have the great potentiality in electronics, optics, mechanics, and biosensing [1,2]. Most applications require individual SWNTs, but the bulk synthesis processes like the electric arc, pulsed laser vaporization, or CVD methods yield SWNTs in the bundled form. Isolated

Address correspondence to V. A. Karachevtsev, B.I. Verkin Institute for Low Temperature Physics and Engineering, Kharkiv 61103, Ukraine. E-mail: karachevtsev@ilt.kharkov.ua

SWNTs can be obtained by sonicating as-prepared SWNT bundles in a water solution of surfactants [3,4] or polymers [5,6]. Intense sonication overcomes the large intertube van der Waals attraction, and free surfactant molecules adsorb to SWNT surfaces and create the micelles around a tube, which prevents the SWNTs reaggregation. Sonication of an aqueous SWNT suspension containing a polymer can also lead to debundled isolated SWNTs. As was shown, DNA is wrapped around the nanotube under sonication and provides a stable aqueous suspension [5,6]. DNA employed in this process opens the door for applications of carbon nanotubes in different fields of bionanotechnology, for example, in genosensing, in medicine, or in the assistance of the SWNTs incorporation into desired molecular architectures. In those developments, a question arises about keeping the stability of the prepared SWNTs:DNA suspension and the prevention of the nanotubes precipitation or, on the contrary, about using the nanotubes aggregation to create a self-assembly [7,8]. DNA can facilitate the application of nanotubes in technology, because this polymer has an excellent molecular recognition capability which is applied widely in many strategies for developing DNA-based nanostructures [9].

There are various ways to intensify the nanotubes aggregation in water: by destruction of micelles or by taking the polymer off from the nanotubes surface, using metal ions [10], dyes [11], changing the suspension pH [3,12], or DNA hybridization [11]. The last can be applied to the directed nanotubes aggregation and the creation of self-assembly structures which can be used for different purposes [7,8].

Herein, we report our work on studying the aggregation of poly(rA)-wrapped single-walled carbon nanotubes, induced by hybridization of the adsorbed polymer with complementary free poly(rU). Differential UV absorption spectroscopy, NIR (near infra-red) luminescence, and AFM were employed for this purpose. In these investigations, we selected relative long homopolynucleotides which provide a high probability of the linking of two polymers because any contact of the polymer leads to the hybridization with complementary one.

2. EXPERIMENTAL DETAILS

Samples Preparation

To study the influence of polymer hybridization on the nanotubes aggregation, potassium salts of poly(rA) (Serva, Germany) and poly(rU) (Sigma-Aldrich, USA) were selected as complementary polynucleotides. The polymers were dissolved in $0.005\,\text{mole}\cdot\text{l}^{-1}$ Na^+ cacodylate buffer (pH 7) (Serva, Germany) with $0.005\,\text{mole}\cdot\text{l}^{-1}$

NaCl. Deionized water with 18 MΩ resistance was used in the experiments.

HipCO-produced single-walled carbon nanotubes were purified by controlled thermal oxidation followed by the HCl treatment [15]. A steady aqueous suspension of SWNTs was prepared by the sonication of nanotubes bundles in buffer with poly(rA) for 40 min (1 W, 44 kHz). Then the solution was centrifuged at 120 000 g for 40 min. Our electrophoretic estimation of the polymer fragmentation after the 40-min sonication gave the length of fragments within 80–150 nucleotides. The initial nanotubes concentration was 0.1 mg/ml. The SWNTs: poly(rA) (poly(rA)^{NT}) concentration ratio was 1:1. After the ultracentrifugation, the supernatant was decanted and dialyzed (dialysis tubing with a molecular weight cutoff of 13–14 kDa) against the buffer solution for 36 h to remove free polynucleotides which did not adsorb to SWNTs. The homogenous suspension of poly(rA)^{NT} was stable for months.

The poly(rA)^{NT} · poly(rU) duplexes formation was achieved after mixing the equimolar amounts of fragmented poly(rU) in buffer with poly(rA) adsorbed to the nanotube surface as well as with the free poly(rA) (Fig. 1) (at room temperature).

Methods

NIR luminescence Spectra of semiconducting carbon nanotubes were recorded by a vis-NIR spectrometer with signal detection by a thermo-cooled InGaAs photodiode (900–1600 nm). Luminescence was excited with a diode-pumped solid-state green laser ($\lambda_{exc} = 532$ nm, 30 mW).

Differential UV-visible absorption spectroscopy was used for the analysis of structural changes in polynucleotides at their interaction with carbon nanotubes. Temperature dependences of changes in the

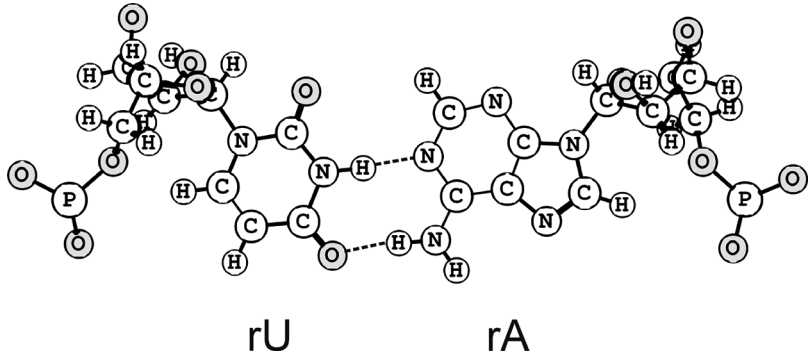

FIGURE 1 Hybridized A-U structure with the Watson–Crick base pairing.

optical density ($\Delta A(T)$) of polynucleotides (the melting curves) were measured with a Specord UV VIS spectrophotometer (Carl Zeiss, Jena, Germany) using a two-cell differential arrangement – one in each channel of the spectrophotometer. Both the cells contained the identical concentration of polynucleotide solutions or poly(rA)^{NT} suspensions which did not exceed 20 μg/ml. The reference cell was thermostatted within $(15 \pm 0.5)^{\circ}$C, the working one was heated at a rate of 0.25 deg/min. The melting curves $h(T)$ of polynucleotides (free or adsorbed to nanotubes) were recorded at $\nu_{max} = 38\ 500\ cm^{-1}$.

Atomic Force Microscopy Experiments

AFM images for biopolymer-wrapped SWNTs were obtained by using a NanoScope III D3000 AFM (Digital Instruments, Santa Barbara, USA) in the Tapping mode™. The measurements were fulfilled by silicon tips (from NT-MDT, Russia) with the nominal apex radius ~10 nm. 7 μl of a diluted suspension of SWNTs:poly(rA) or SWNTs: poly(rA)^{NT} · poly(rU) hybrids were placed onto a freshly cleaved mica surface by the spin-coating method. Then the sample was air-dried and analyzed by AFM.

Molecular Dynamic Simulation

The formation of poly(rA):SWNT bionanohybrid was simulated by the molecular dynamic method. In our simulation, the program package NAMD [16] was employed with Charmm27 force field parameter set [17,18]. During the simulation, a box was applied, being of $55 \times 55 \times 135$ Å dimensions, in which poly(rA)^{NT} was embedded in water (more than 9000 H_2O molecules). In all the cases, SWNT was selected as a zigzag (16.0) carbon nanotube. Its length and diameter were 11.0 nm and 1.27 nm, respectively. The 30-nucleotides length of poly(rA) was selected for our simulation. Before the optimization procedure, we chose backbone torsion angles of poly(rA) in such a manner that the direction of the polymer axis was 45° with respect to the nanotube one. This angle was determined experimentally in circular dichroism measurements [19]. To neutralize the charge on the sugar-phosphate backbone, 30 Na^+ ions were added close to the polymer. Such a system was optimized and then modeled during 0.5 ns (with a 1-fs time step). The visual analysis of the structure obtained after the modeling showed that about a half of adenines were in the π-π stacking with the nanotube surface and, other adenines were out of the stacking with the SWNT surface, and some of them formed a self-stacking. The distance between stacked bases and the tube surface was about 3.4–3.5 Å. To simulate the polymers hybridization,

we located poly(rU) (30-nucleotides) close to the optimized poly(rA): SWNT and then optimized this hybrid again. Modeling temperature and pressure in the periodic box were 293 K and 1bar, respectively.

3. RESULTS AND DISCUSSION

The absorption spectrum of bionanohybrids formed with poly(rA) adsorbed to SWNTs and poly(rU) in the aqueous suspension in the range of wavenumbers $(14–46) \cdot 10^3\,cm^{-1}$ is conditioned by contributions both of polymers and SWNTs (Fig. 2). A wide band at $(36–42) \cdot 10^3\,cm^{-1}$ and the following absorption rise in the high-frequency fields are caused by the poly(rA)poly(rU) absorption, namely, by the absorption of nitrogen bases. The monotonic absorption growth from red up to UV is mainly associated with the absorption of nanotubes, whose spectrum in the aqueous suspension with SDS (this surfactant does not absorb a light in the observed spectral range) is shown in Figure 2 as well.

Upon the formation of the ordered double helical structure from two individual strands (Fig. 1), the optical absorption of this double-stranded polymer becomes less than the sum of two polymers

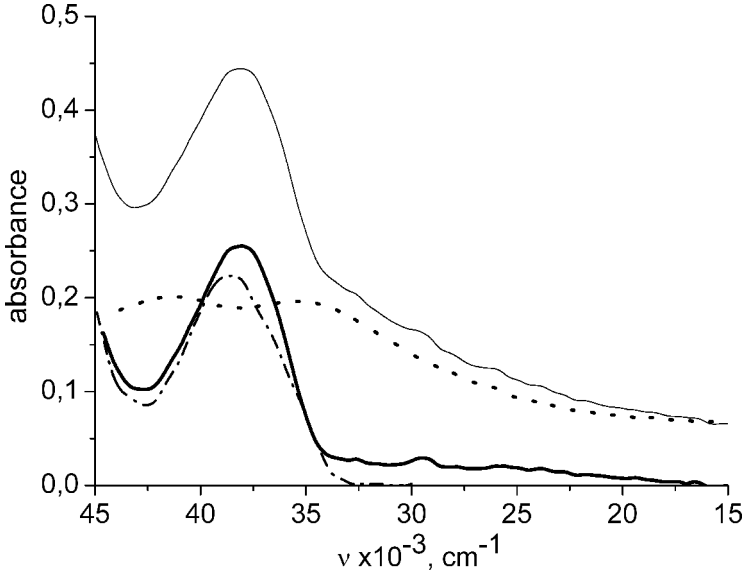

FIGURE 2 UV-visible absorption spectra of a poly(rA)^{NT} aqueous suspension (thin curve), and an SWNTs aqueous suspension with SDS (1 wt.%) (dotted curve), the differential spectrum of poly(rU)poly(rA) adsorbed to the SWNT surface (bold curve), and the spectrum of free poly(rU)poly(rA) (broken curve).

absorptions because of the hypochromic effect caused by the stacking interaction among nitrogen bases [20]. Quantitatively, this effect can be characterized by h (hyperchromic coefficient) calculated as $h = \Delta A/A_0$ where A_0 is the optical absorption of the ordered polymer and ΔA is a difference in the absorptions of partially disordered (A) and ordered polymers ($\Delta A = A - A_0$). The poly(rU) hybridization with poly(rA)^{NT} is also manifested in a decrease of the total UV light absorption. The essential part of complementary pairs is formed during the mixing of two solutions and for following 100–200 sec. Then the process slows down significantly. This observation is in agreement with the result of the kinetic study on the relative short oligomers hybridization, in which a slower hybridization on SWNTs was observed too [21]. To confirm the creation of the double-stranded conformation, we measured the melting curves of poly(rA) · poly(rU) formed on SWNTs in 6 h after the mixing of the initial solutions (Fig. 3, curve 1). The temperature dependence of the change in the optical absorption has S-like form which is characteristic of the helix-coil transition in double-stranded polymers. The melting curve 1 (Fig. 3) has a bending in the interval 33–38°C dividing the whole curve into two parts which can be attributed to two polymer structures with different thermal stabilities. We suppose that the heterogeneity in the poly(rU) · poly(rA)^{NT} structure is a result of the

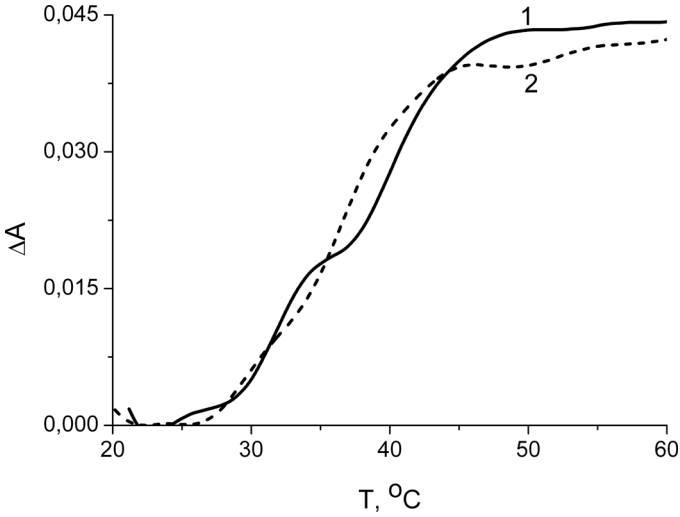

FIGURE 3 Melting curves (measured at $\nu = 38\,500\,\text{cm}^{-1}$) of fragmented poly (rU) · poly(rA)^{NT} formed after the 6-h hybridization (bold) and after 7 days (broken).

polymers interaction with the nanotube surface, which hampers the hybridization along the whole polymer length. In this case, a part of bases does not take part in the hybridization at all, and other one forms defective base pairs, for example, with one H-bond, or hybridized pairs have no optimal energy structure. The double polymer having a greater number of hybridization defects will be of lower thermal stability. With the couse of time, the transition curve becomes smoother (Fig. 3, curve 2, obtained in 7 days after the mixing of the initial solutions) and is characterized with the melting temperature $T = 37^{\circ}C$. It is obvious that the hybridization of the polymers adsorbed to the nanotube is a rather slow process and proceeds for some days. It should be noted that the melting temperature of the double-stranded polymer formed on a nanotube is lower than that of the free polymer, which is 44°C [21].

Poly(rA)-wrapped semiconducting nanotubes emit in the NIR spectral range (Fig. 4a). Spectral features are attributed to individual SWNTs of certain diameters [22], in which the band gap transitions occur between the first pair of Van Hove singularities in the density of states of semiconducting SWNTs. We fitted of the experimental spectrum with the sum of 12 Lorentzian curves (Table 1). After the mixing of poly(rU) with poly(rA)^{NT} and a few (5–6) hours of hybridization, the emission of the solution was reduced by 10–15%. We believe that this emission decrease is caused by the appearance of light scattering because of the nanotubes aggregation induced by the polymers hybridization. This suggestion correlates with UV light absorption measurements (see below). After the hybridization, the bands shifted slightly (not above 3 meV) in a low-frequency field (Table 1). This result differs from that of Prof. M. Strano's group research [24], in which a blue shift of bands of the nanotubes emission spectrum was observed after the hybridization of two short complementary oligonucleotides on the tube surface. This shift was explained with a decrease of the tube surface area contacted with water due to the extension of the nanotube surface coating by the double-stranded hybridized polymer. In the experiment, the initial fractional coverage of SWNT by single-stranded DNA did not exceed 0.25, and the final coverage was 0.5. However, in our case, as follows from the AFM image (Fig. 5), almost all the surface of nanotubes (except the tube ends) was covered with poly(rA), and an additional reduction of the tube surface contacted with water should not be expected. In this figure, the heights of wire-like structures are not above 2.0–2.4 nm. As the height of single-stranded DNA on the surface is 0.8–1.2 nm [24,25], and the tubes diameter has a distribution mainly from 0.8 to 1.4 nm [23], we can make conclusion that the wire-like

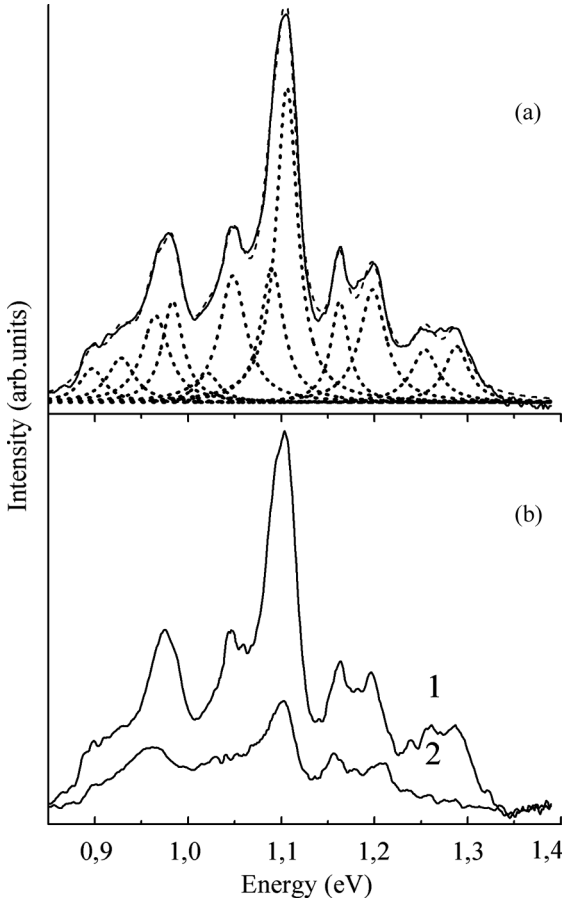

FIGURE 4 Emission spectra of semiconducting nanotubes in an aqueous solution with the poly(rA) surrounding (a) obtained in 4 h (broken lines are Lorentzian curves fitted to the experimental spectrum), (b) two days (1), and one month (2) after the poly(rU) addition.

structures are individual nanotubes covered by the polymer. It is obvious that some tens of polymer fragments with a length of 30–50 nm are necessary to cover the whole tube surface, the lengths of which are in the interval 0.5–1 μm.

The red shift of the nanotubes emission bands observed in the course of time after the polymer hybridization (Fig. 4b) can be explained by the partial release of the nanotube surface from the polymer and by an increase of the contact area of this surface with water. The polymer release from the nanotube surface as a result of the

TABLE 1 Spectral position (E, eV), relative area, and full-width ($\Delta\Gamma$) at half-maximum (FWHM) intensity of Lorentzians used to fit the emission spectra of a semiconducting nanotubes aqueous suspension with the poly(rA) or poly (rA) · poly(rU) surrounding. ΔE (meV) is a spectral shift of the bands in the spectrum as a result of the hybridization, (n, m) denotes the nanotube chirality indices [22]

SWNTs:poly(rA)		SWNTs:poly(rA) poly(rU)			
Energy, eV	Area	Energy, eV	Area	ΔE, mev	(n,m)
0.897	3	0.895	4	2	12.2
0.928	5	0.926	6	2	9.7
0.965	8	0.965	9	0	11.1
0.983	8	0.983	7	0	10.3
1.021	2	1.019	2	3	11.3
1.048	13	1.048	13	0	8.6
1.090	10	1.089	13	1	8.4
1.106	23	1.106	17	0	9.4
1.163	7	1.162	8	1	10.2
1.198	11	1.198	10	0	7.5
1.254	5	1.254	5	0	6.5
1.288	5	1.286	6	2	8.3

polymer hybridization was observed earlier in [11], in which the hybridization of oligoA_{30} with complementary oligomers of the same length (oligoT_{30}) adsorbed to the nanotube is followed by the nanotubes precipitation.

The AFM image demonstrates branched nanotube structures which were formed in an aqueous suspension of SWNTs with poly(rA) (Fig. 5). These structures can appear if a relatively long polymer is adsorbed to two individual nanotubes. The number of such branched structures increases with adding poly(rU) into the suspension. Two ends of this polymer can bind to complementary strands of poly(rA) adsorbed to different individual tubes. In our case, the efficiency of such an aggregation increases, as any local contacts of two polymers may result in the hybridization. With time, the dimension of these structures increases, yielding the SWNTs precipitation: as a result, the nanotubes emission is quenched (Fig. 4b).

A possible structure of poly(rU) hybridized with two SWNTs covered with poly(rA) was simulated by the molecular dynamic method and is presented in Figure 6. The detailed analysis of two polynucleotides contacts shows that uraciles of poly(rU) form different types of H-bonds with components of poly(rA), create stacking dimers with adenine, and some of them interact with the nanotube surface.

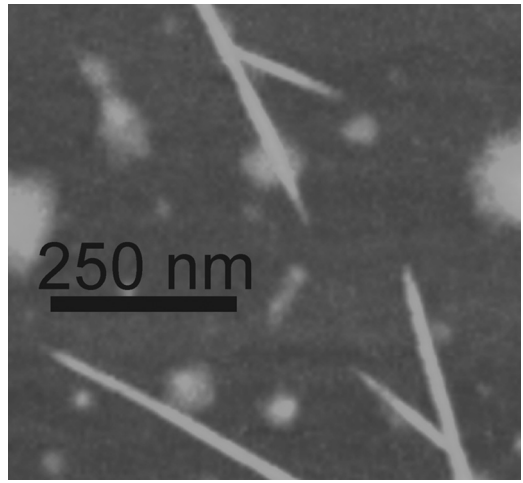

FIGURE 5 AFM image of poly(rA)^{NT} hybrids on the mica substrate.

We observed also the appearance of light scattering in UV-visible absorption measurements, in which the light transmission of the SWNTs suspension with a hybridized polymer was decreased. When

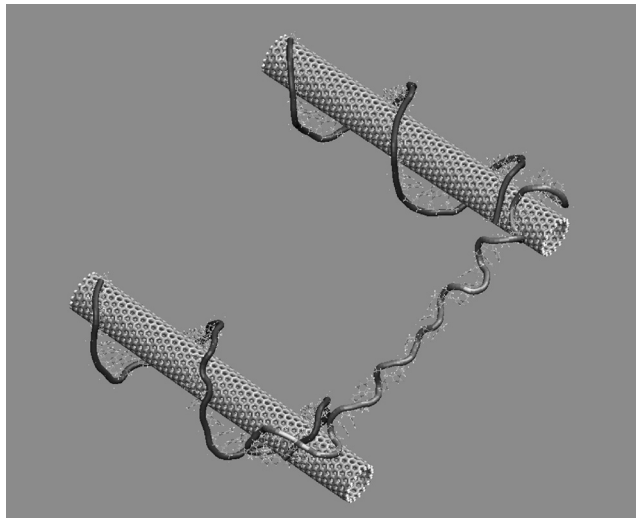

FIGURE 6 Computer modeling of a poly(rU)$^{+}$poly(rA)^{NT} hybrid. Two nanotubes with wrapped poly(rA) are sewed by free poly(rU). Water molecules were extracted for the better visualization. Bold line shows the arrangement of the sugar-phosphate backbone around a tube.

we subtracted the spectrum of SWNTs suspension with SDS from the absorption spectrum of poly(rA)^{NT}poly(rU), we obtained the spectrum of polymer [$(36–42) \cdot 10^3\,cm^{-1}$] and a monotonic decrease of the absorption in the low-frequency range (long tail) caused by the light scattering (Fig. 2, bold line). We revealed also that the light transmission of the poly(rA)^{NT}poly(rU) suspension in UV and visible ranges decreases with time because of a rise in the light scattering. Using the standard approach [26], we evaluated the mean size of aggregates and its change in time. This method allows one to estimate the aggregate size by the slope of the optical absorption change as a function of the wavelength on the double logarithmic scale. So, according to these

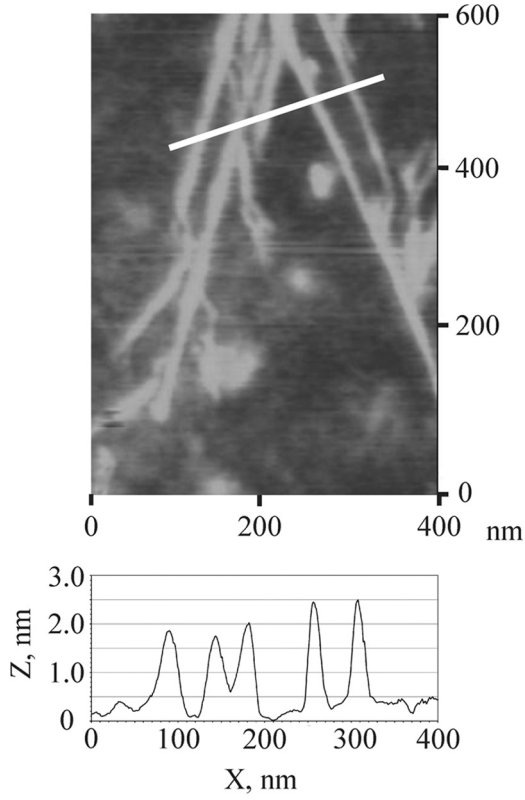

FIGURE 7 AFM image of poly(rU)poly(rA)^{NT} aggregates on the mica substrate. Line scans (along the white line from left to right) shown in boxes reveal that the height of a SWNT with the polymer adsorbed varies from 1.8 to 2.5 nm.

estimates, the mean size of the aggregate became by 2.5 times bigger for 7 days – from 46 to 106 nm. Though the equations we used were derived for spherical particles and do not provide the real size of aggregations exactly, however, these relative values show a rise of the aggregate size with time.

Thus, in 2 weeks, the luminescence intensity decreased more than two times (Fig. 4). Then, after 3 weeks, we observed the nanotubes precipitation. Such aggregated structures can be seen by AFM on a mica substrate obtained after the deposition from the aqueous suspension (Fig. 7). The AFM image cross-section analysis of poly(rA)^{NT} poly(rU) revealed that the height of hybrid structures ranges from 1.8 to 2.5 nm. Such heights indicate that the wire-like structures observed in the AFM image correspond to individual nanotubes. With time, the nanotubes aggregates size increases, and, after reaching the critical size, such aggregates precipitate. This process can be observed visually in the optical cell or by measuring the nanotube luminescence intensity which decreases with time. Because the poly(rA)^{NT} suspension is stable for months, and poly(rA)^{NT}poly(rU) suspension is stable only for weeks, we believe that the nanotubes precipitation is related to the polymers hybridization.

CONCLUSION

The hybridization of poly(rA) adsorbed to the nanotube surface with free complementary poly(rU) leads to the formation of a double-stranded polymer, the appearance of which is confirmed with the characteristic *S*-like form of its melting curve. The melting curve has a bending, dividing the whole curve into two temperature ranges, every of which can be attributed to one of these two polymer structures with different thermal stabilities. The heterogeneity of the poly(rU)$\cdot$ poly(rA)^{NT} structure is a result of the polymers interaction with the nanotube surface, which hampers the regular hybridization along the whole polymer length. In a week, the transition curve becomes smoother, and this means that the hybridization of the polymers adsorbed to the nanotube is a rather slow process and proceeds for some days. The hybridization of poly(rA) adsorbed to the nanotube surface with free poly(rU) induces the aggregation of nanotubes. At hybridizing free poly(rU) with two complementary poly(rA) adsorbed to different individual tubes, their local cross-linking occurs. The nanotubes aggregation is accompanied with the light scattering and can be observed by AFM. The size of the assembly increases with time, and then this process results in the nanotubes precipitation.

REFERENCES

[1] Jagota, A., Diner, B. A., Boussad, S., & Zheng, M. (2005). Carbon nanotube-biomolecule interactions: Applicatons in carbon nanotube separation and biosensing. In: *Applied Physics of Nanotubes: Fundamentals of Theory, Optics and Transport Devices*, Rotkin, S. V. & Subramoney, S. (Eds.), Springer: Berlin-Heidelberg, Ch. 10, p. 253–272.

[2] Kichambare, P. D. & Star, A. (2007). Biosensing using carbon field-effect transistor. In: *Nanomaterials for Biosensors*, Challa S. S. R. Kumar (Ed.), Wiley-VCH, Ch. 1, p. 1–26.

[3] Strano, M. S., Huffman, C. B., Moore, V. C., O'Connell, M. J., Haroz, E. H., Hubbard, J., Miller, M., Rialon, K., Kittrell, C., Ramesh, S., Hauge, R. H., & Smalley, R. E. (2003). *J. Phys. Chem. B*, *107*, 6979.

[4] O'Connell, M. J., Bachilo, S. M., Huffman, C. B., Moore, V. C., Strano, M. S., & Haroz, E. H. *et al.* (2002). *Science*, *297*, 593.

[5] Zheng, M., Jagota, A., Semke, E., & Diner, B. *et al.* (2003). *Nature Materials*, *2*, 338.

[6] Zheng, M., Jagota, A., Strano, M., Santos, A., Barone, P., & Chou, S. *et al.* (2003). *Science*, *302*, 1545.

[7] Li, S., He, P., Dong, J., Guo, Z., & Dai, L. (2005). *J. Am. Chem. Soc.*, *127*(1), 14.

[8] Chen, Y., Haipeng, L., Tao, Y., Junghwa, K., & Chengde, M. (2007). *J. Am. Chem. Soc.*, *129*(28), 8696.

[9] Young Sun & Kiang, C.-H. (2005). DNA-based artificial nanostructures: Fabrication, properties, and applications. In: *Handbook of Nanostructured Biomaterials and Their Applications in Nanobiotechnology*, Nalwa, H. S. (Ed.), American Scientific Publishers, Vol. 2, Ch. 12, p. 224–246.

[10] Niyogi, S., Boukhalfa, S., Chikkannanavar, S. B., McDonald, T. J., Heben, M. J., & Doorn, S. K. (2007). *J. Am. Chem. Soc.*, *129*(7), 1898.

[11] Chen, R. J. & Zhang, Y. (2006). *J. Phys. Chem. B*, *110*, 54.

[12] Karachevtsev, V. A., Glamazda, A. Yu., Leontiev, V. S., Mateichenko, P. V., & Dettlaff-Weglikowska, U. (2005). In: *AIP Conference Proceedings*, Kuzmany, H., Fink, J., Mehring, M., & Roth, S. (Eds.), American Institute of Physics Melville, NY, Vol. 786, 257.

[13] Holcomb, D. N. & Timasheff, S. E. (1968). *Biopolymers*, *6*, 513.

[14] Sorokin, V. A., Valeev, V. A., Gladchenko, G. O., Degtyar, M. V., Karachevtsev, V. A., & Blagoi, Yu. P. (2003). *Int. J. Biol. Macromol.*, *31*, 223.

[15] Dettlaff-Weglikowska, U., Benoit, J.-M., Chiu, P.-W., Graupner, R., Lebedkin, S., & Roth, S. (2002). *Curr. Appl. Physics*, *2*, 497.

[16] Phillips, C., Braun, R., Wang, W., Gumbart, J., Tajkhorshid, E., Villa, E., Chipot, Ch., Skeel, R. D., Kale, L., & Schulten, K. (2005). *J. Comp. Chem.*, *26*, 1781.

[17] MacKerell Jr., A. D., Bashford, D., Bellott, M., Dunbrack, R. L., Jr., Evanseck, J. D., & Field, M. J. *et al.* (1998). *J. Phys. Chem. B*, *102*, 3586.

[18] Foloppe, N. & MacKerell, Jr. A. D. (2000). *J. Comp. Chem.*, *21*, 86.

[19] Rajendra, J. & Rodger, A. (2005). *Chem. Eur. J.*, *11*, 4841.

[20] Cantor, C. R. & Schimmel, P. R. (1980). *Biophysical Chemistry*, Part II, Freeman: San Francisco.

[21] Jeng, E. S., Barone, P. W., Nelson, J. D., & Strano, M. S. (2007). *Small*, *3*(9), 1602.

[22] Krakauer, H. & Sturtevant, J. (1968). *Biopolymers*, *6*, 491.

[23] Weisman, R. B. & Bachilo, S. M. (2003). *Nano Lett.*, *3*(9), 1235.

[24] Jeng, E. S., Moll, A. E., Roy, A. C., Gastala, J. B., & Strano, M. S. (2006). *Nano Lett.*, *6*, 371.

[25] Karachevtsev, M. V., Lytvyn, O. S., Stepanian, S. G., Leontiev, V. S., Adamowicz, L., & Karachevtsev, V. A. (2008). *J. Nanoscience and Nanotechnology*, *8*, 1473.

[26] Allen, T. (1990). *Particle Size Measurement*, Chapman & Hall: London.